

RESEARCH PAPER



## YB-3 substitutes YB-1 in global mRNA binding

D. N. Lyabin <sup>a\*</sup>, I. A. Eliseeva<sup>a\*</sup>, E. A. Smolin<sup>a</sup>, A. N. Doronin<sup>a,b,c</sup>, K. S. Budkina<sup>a</sup>, I. V. Kulakovskiy<sup>d,e,f</sup>, and L. P. Ovchinnikov<sup>a</sup>

<sup>a</sup>Institute of Protein Research, Russian Academy of Sciences, Pushchino, Russia; <sup>b</sup>Department of Bioengineering, BIOCAD, Lyubuchany, Russia; <sup>c</sup>Faculty of Molecular and Cellular Biotechnology, Pushchino State Institute of Natural Science, Pushchino, Russia; <sup>d</sup>Vavilov Institute of General Genetics, Russian Academy of Sciences, Moscow, Russia; <sup>e</sup>Engelhardt Institute of Molecular Biology, Russian Academy of Sciences, Moscow, Russia; <sup>f</sup>Institute of Mathematical Problems of Biology RAS - the Branch of Keldysh Institute of Applied Mathematics, Russian Academy of Sciences, Pushchino, Russia

### ABSTRACT

Y-box binding proteins are DNA- and RNA-binding proteins with an evolutionarily ancient and conserved cold shock domain. The Y-box binding protein 1 (YB-1) is the most studied due to its abundance in somatic cells. YB-1 is involved in a variety of cellular processes, including proliferation, differentiation and stress response. Here, using Ribo-Seq and RIP-Seq we confirm that YB-1 binds a wide range of mRNAs and globally acts as a translation inhibitor. Surprisingly, *YBX1* knockout results in only minor alterations in the expression of other genes, mostly caused by changes in RNA abundance. But *YB-3* mRNA is an exception: it is better translated in the absence of YB-1, thereby producing an increased amount of YB-3 and thus suggesting that its synthesis is under YB-1 negative control. We have shown that the set of mRNAs bound to YB-3 is strikingly similar to that of YB-1, and that the mRNA-binding by YB-3 is enhanced in the absence of YB-1, resulting in a similar global reduction of translation of bound mRNAs in YB-1-null cells. Thus, YB-3 acts as a substitute for YB-1 in mRNA binding and, probably, in global translational control.

### ARTICLE HISTORY

Received 27 August 2019  
Revised 8 December 2019  
Accepted 23 December 2019

### KEYWORDS

YB-1; YBX1; YB-3; YBX3;  
Ribo-Seq; RIP-Seq;  
translational control

## Introduction

Y-box binding proteins drew researchers' close attention in the late eighties of the last century. Today, the best-studied member of this family is YB-1, whose multiple cellular functions and involvement in proliferation, differentiation, and stress response have been recognized [1]. It remains controversial by what mechanism it acts and which stages of the gene expression it regulates.

As known, YB-1 is involved in DNA replication, DNA repair, and pre-mRNA alternative splicing; also, its post-secretion extracellular functions (mRNA sorting, Notch binding) have been recognized [2,3]. However, the most important and the most studied functions of YB-1 are regulation of transcription and translation [2].

In transcription, YB-1 has been shown to act both as an activator or inhibitor, but the reported evidence is mostly indirect [1]. Currently, a comprehensive set of all YB-1 targets at the transcriptional level is not available, since neither the canonical Y-box motif nor any other clear motif is enriched in YB-1-bound genomic regions [1,4]. Probably, the lack of predominant sequence patterns is associated with a huge number of protein partners capable of interacting with YB-1 due to its structural intrinsic disorder.

In translation, the YB-1 functions are known in more detail. Initially, YB-1 was recognized as a global translation regulator

that, at a high YB-1/mRNA ratio, inhibits translation by displacing the translation initiation complex eIF4F from the cap-structure of any mRNA. Concurrently, YB-1 packages mRNAs into mRNPs that are unaffected by the cellular mRNA degradation machinery, thereby stabilizing these mRNAs [5,6]. However, most of the data supporting this hypothesis were obtained either using a cell-free translation system or from experiments with purified components *in vitro*.

Later, high-throughput experiments showed that YB-1 predominantly binds to mRNAs whose translation products belong to groups related to proliferation, differentiation, or binding of nucleic acids. It was also demonstrated that over-expression of YB-1 in mammary epithelial cells MCF10AT with the activated Ras-MAPK signaling pathway results in activation of translation of a whole class of mRNAs encoding transcription factors necessary for the epithelial-mesenchymal transition. Presumably, the translation of these mRNAs with highly structured 5' UTRs is performed by a cap-independent mechanism requiring an elevated concentration of YB-1 [7].

The results of knockout experiments are not fully clear. On the one hand, *YBX1* knockout in mice results in normal embryonic development for 13.5 days followed by a sudden drop in the embryo growth rate, anomalies in the neural tube formation, and prenatal death of the animals [8]. On the other hand, analysis of mouse embryonic fibroblasts isolated from

**CONTACT** D. N. Lyabin  [lyabin@vega.protres.ru](mailto:lyabin@vega.protres.ru); L. P. Ovchinnikov  [ovchinn@vega.protres.ru](mailto:ovchinn@vega.protres.ru)  Institute of Protein Research, Russian Academy of Sciences, Institutskaya4, Pushchino 142290, Russia

\*Joint first authors.

 Supplemental data for this article can be accessed [here](#).

YB-1<sup>-/-</sup> embryos revealed no serious changes in transcription and total protein synthesis [8].

We applied high-throughput sequencing to analyse the translome (with ribosome profiling, Ribo-Seq) and YB-1-associated fraction of the transcriptome of HEK293T cells, including YB-1 overexpression and CRISPR/Cas9 knockout. In wild type and YB-1-overexpressing HEK293T cells, YB-1 acted as a global translation inhibitor. However, in YB-1-null cells, we observed only minor changes in gene expression, mostly at the transcriptional level. A notable exception was the YB-3 mRNA exhibiting better translation and resulting in a higher amount of the synthesized protein and thus suggesting that the YB-3 overexpression was the compensation for the absence of YB-1. This hypothesis was supported by mRNA-immunoprecipitation sequencing (RIP-Seq) revealing that YB-1 and YB-3 shared a similar set of bound mRNAs and that the mRNA-binding by YB-3 was enhanced in the absence of YB-1.

## Results

### YB-1 globally acts as a translation inhibitor

One of the many putative functions of YB-1 is the global translational control [2]. We performed ribosomal profiling (Ribo-Seq) and RNA immunoprecipitation followed by deep sequencing (RIP-Seq) of HEK293T cells to assess the relationship between ribosome occupancy and YB-1-binding efficiency at the transcriptome-wide scale.

At comparable sequencing depth of RNA-Seq and RIP-Seq, the read counts from those are well-correlated (Pearson's correlation coefficient from 0.49 to 0.89 depending on antibodies and rRNA depletion protocol, Supplementary Fig. S1A). For more than 80% of expressed genes, respective transcripts are detected in the YB-1-bound transcriptome fraction. Thus, YB-1 should be considered as a universal RNA-associated protein capable of binding a very wide range of RNAs.

Next, we estimated the ribosome occupancy at gene coding segments (CDS) as the normalized Ribo-Seq read counts relative to the normalized read counts of the size-matched RNA-Seq samples, and the YB-1 immunoprecipitation efficiency as YB-1 RIP-Seq normalized read counts for the whole transcripts relative to those from standard RNA-Seq samples.

By comparing the ribosome occupancy at CDS and YB-1 immunoprecipitation efficiency we found a weak significant negative correlation (Pearson's  $CC = -0.14$ ,  $P < 10^{-15}$ ), with even the stronger effect (Pearson's  $CC = -0.23$ ,  $P < 10^{-15}$ ) upon YB-1 overexpression (Fig. 1A). Thus, YB-1 binds the major fraction of the transcriptome and its binding is negatively associated with the mRNA translation efficiency. This agrees with the published data obtained in the cell-free translation systems [6,9], where YB-1 served as a non-specific translation inhibitor.

Of note, both observations are consistent for RIP-Seq results from two different YB-1 antibodies (Supplementary Fig. S1B).

### YBX1 knockout leads to limited changes in the translome

High-throughput data provided evidence for YB-1 as a global translation inhibitor. However, an analysis of the global translation level in murine embryonic fibroblasts showed virtually no changes upon *YBX1* knockout [8]. To clarify this discrepancy, we generated a YB-1-null HEK293T cell line (HEK293TΔYB-1) using the CRISPR/Cas9 genome editing technique (Fig. 1B, Supplementary Text and Supplementary Fig. S2).

The HEK293TΔYB-1 cells had a lower division rate (Fig. 1C), which is in agreement with previous observations that a decreased YB-1 amount results in the decreased cell division rate [10,11]. The HEK293TΔYB-1 cells exhibit altered expression of selected cell cycle markers (Cyclin A2, CDK4, CDK6, Smad1, 3, 4, and CDK inhibitors p18, p21, p27. Supplementary Text and Supplementary Fig. S3). Synthesis of exogenous HA-YB-1 in the HEK293TΔYB-1 cells restored the division rate to the normal level of HEK293T cells (Fig. 1C). Thus, the reduced division rate of HEK293TΔYB-1 cells was indeed caused by the absence of YB-1, and the obtained ΔYB-1 cells provide a valid loss-of-function model.

Next, we tested the effect of *YBX1* knockout on the global translation level in HEK293T cells using metabolic labeling with the methionine analogue azidohomoalanine (Fig. 1D), where the cells were treated with azidohomoalanine, lysed, and the newly synthesized protein was fluorescently labeled by Click Chemistry (see Methods).

The global translation level per cell in case of *YBX1* knockout decreased only slightly, by about 15% (similarly to that observed in [8]). Expression of HA-YB-1 in HEK293TΔYB-1 cells raised the translation level, but only by 5-10% (statistically non-significant). With YB-1 considered to be the general translation inhibitor, the global translation decline upon *YBX1* knockout seems baseless. However, in rabbit reticulocyte lysate, the absence of YB-1 was found to inhibit translation [12]. In the case of knockout cells, this observation suggests that there is a strong compensatory mechanism, which we discuss below.

With only a minor effect on the global translation, a more exhibited change of translation could be expected in HEK293TΔYB-1 for particular mRNAs targeted by YB-1 in HEK293T. We performed Ribo-Seq and size-matched RNA-Seq of HEK293TΔYB-1 cells and compared the results with data for HEK293T. The results of high-throughput experiments were validated using qPCR for 26 genes (Supplementary Text and Supplementary Figs. S4-S5), 8 of those were also verified by the Western-blot analysis (Supplementary Fig. S3).

Fig. 2A presents the correlation between changes in Ribo-Seq and changes in RNA-Seq (Pearson's  $CC = 0.76$ ,  $P < 10^{-15}$ ); here Ribo-Seq and RNA-Seq read counts were obtained for the whole transcripts. Further computational analysis of differential ribosome occupancy between HEK293TΔYB-1 and HEK293T cells with edgeR aimed to reveal translation changes of particular transcripts but detected no statistically significant genes with Benjamini-Hochberg (FDR) adjusted  $P$ -value  $< 0.05$ .

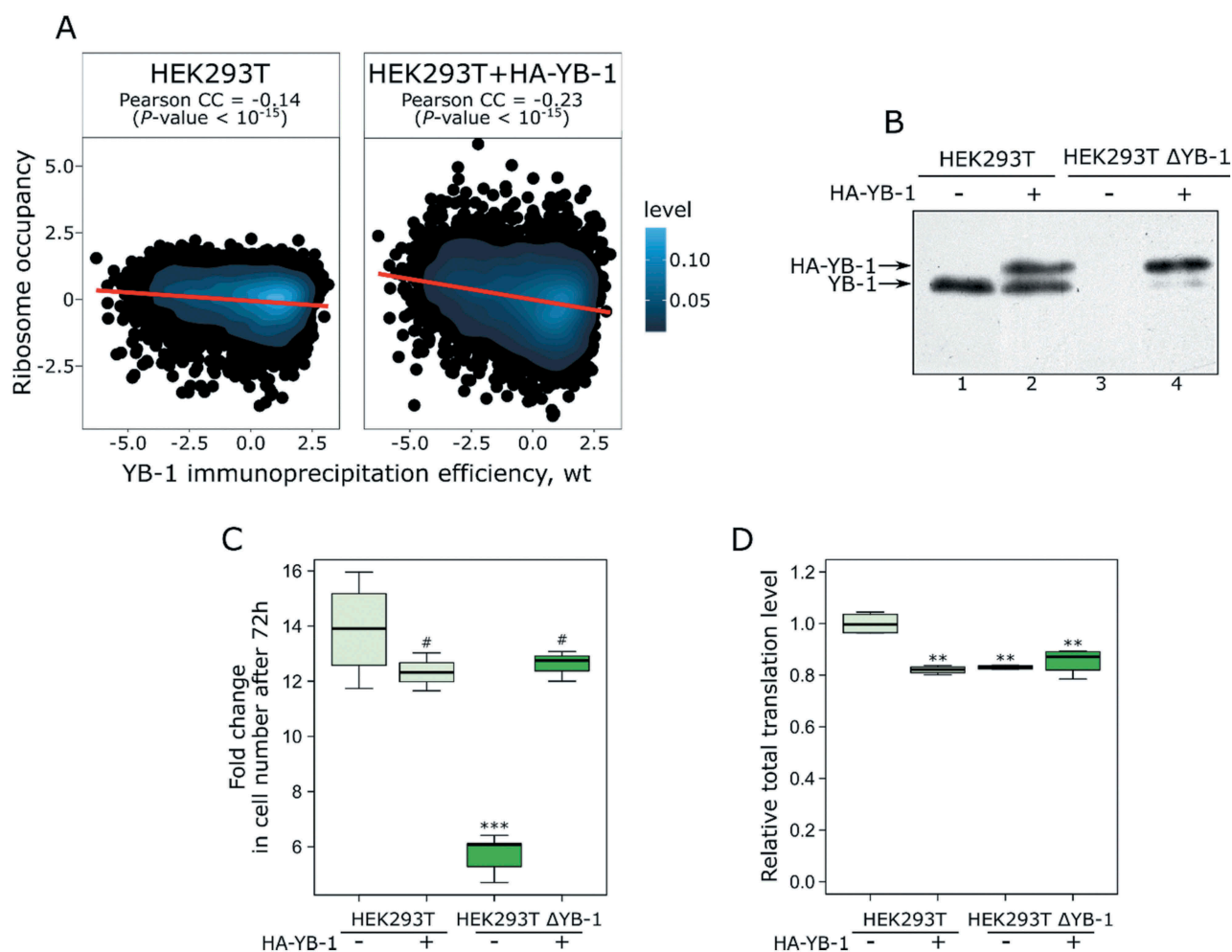


**Figure 1.** *YBX1* knockout leads to reduced cell proliferation and weak global downregulation of translation. (A) Scatterplot of ribosome occupancy in HEK293T (Y-axis, left) or HEK293T overexpressing YB-1 (Y-axis, right) and the YB-1 immunoprecipitation efficiency in HEK293T (X-axis, both panels). The two-dimensional kernel density estimation, the linear regression line, the Pearson's correlation coefficient, and the significance of correlation ( $P$ -value) are shown. For each gene, the ribosome occupancy (Ribo-Seq read counts normalized to the RNA-Seq read counts) was estimated at coding segments, excluding UTRs. (B) Changes in the amount of YB-1 in HEK293T cells after knockout or plasmid-induced expression of YB-1, as revealed by Western blotting. (C) Changes in the number of HEK293T and HEK293T $\Delta$ YB-1 cells after 72 h cultivation. Equal numbers of HEK293T and HEK293T $\Delta$ YB-1 cells after 24h transfection by pcDNA-HA or pcDNA-HA-YB-1 were replated to dishes, and the cell growth was monitored by cell counting over 72 hours. The data represent three independent experiments. (D) The total translation level in HEK293T and HEK293T $\Delta$ YB-1 cells transfected either by the empty vector pcDNA3-HA or pcDNA3-HA-YB-1 (HA-YB-1) was assessed from the incorporation of azido-homoalanine. The values were computed as follows: for each biological replicate, the values were normalized to the mean value of a particular replicate; the obtained values were then normalized across experiments to the mean value of HEK293T cells transfected by the empty vector. Two-tailed Student's  $t$ -test was used to estimate the statistical significance versus HEK293T cells transfected by the empty vector. \*\*\* $p$  < 0.001, \*\* $p$  < 0.01, # – not significant.

Next, we applied the gene set enrichment analysis to the gene lists ranked by changes in RNA-Seq or ribosome occupancy (Ribo-Seq relative to RNA-Seq). This way we found several functional groups of RNAs with ribosome occupancy increased in HEK293T $\Delta$ YB-1. In particular, translation-level changes compensating the reduced mRNA abundance were detected for mRNAs related to the cell cycle and cellular respiration (Fig. 2C). This was typical for other significant gene ontology terms and functional groups (Supplementary Table S2).

However, there was a notable exception: genes of cell response to growth factor stimulus, including those of TGF- $\beta$ -signaling, were upregulated at the transcriptional level and slightly at translational level. This is of special interest since YB-1 is known to act as an antagonist in TGF- $\beta$ -signaling to some extent [13,14] and, furthermore, YB-1 and TGF- $\beta$  counter-regulate each other [15,16].

To sum up, we were unable to detect particular genes with statistically significant translation-level changes but found multiple significant functional gene groups, which exhibited slight but orchestrated changes. This suggests an active compensatory mechanism activated in the YB-1 absence.

### *YB-1 controls YB-3 expression*

While no genes showed statistically significant changes at the translational level in HEK293T $\Delta$ YB-1 cells, there were a few outliers (see the volcano-plot, Fig. 2B) of which there were no RNA-binding or translation-related proteins, except for YB-3, which showed the most significant increase of the mRNA translation level. YB-3 is a homolog of YB-1 that was speculated to have overlapping functions, as follows from the survival of YB-1-null mouse embryos [17].

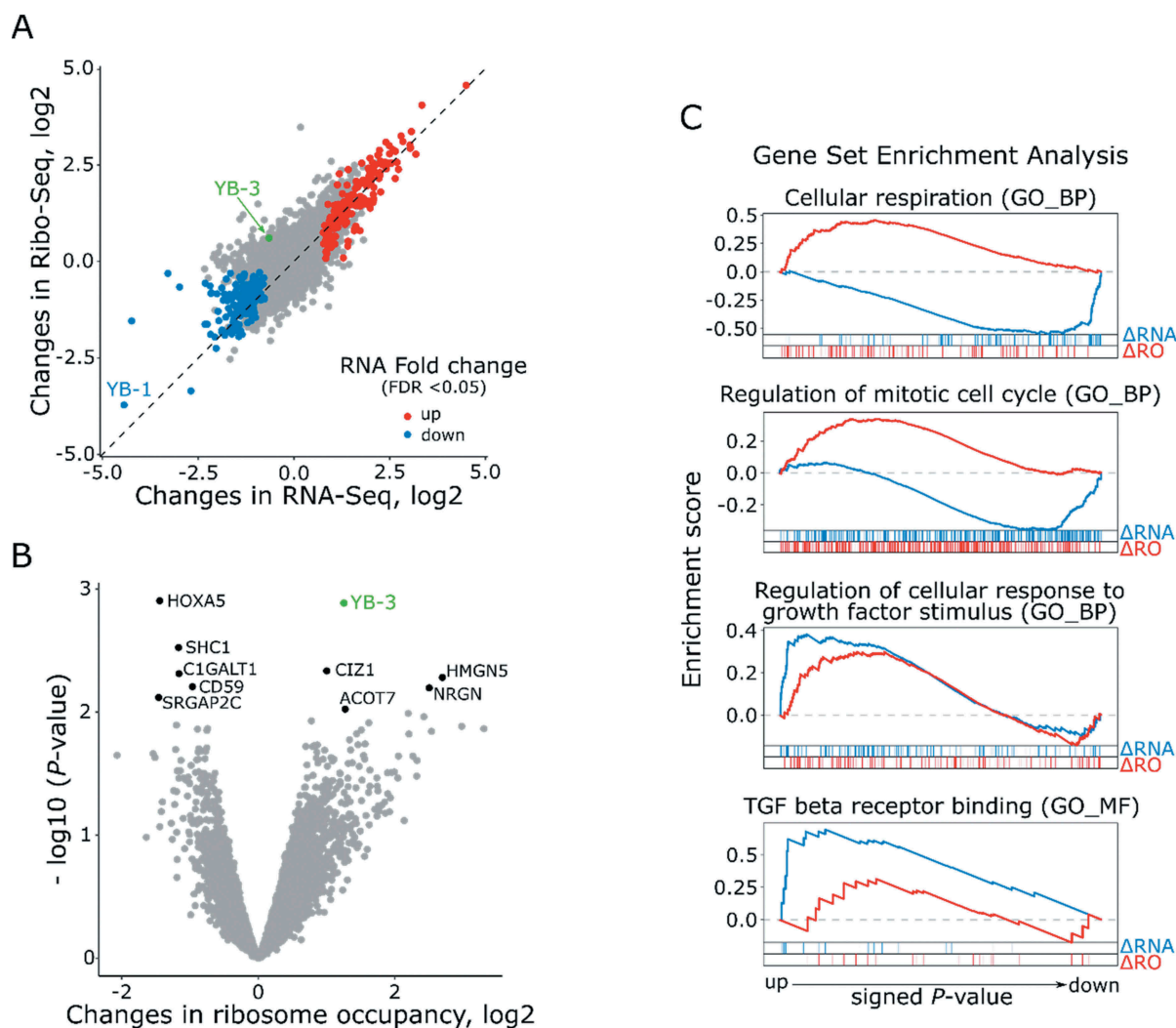


**Figure 2.** *YBX1* knockout leads to limited changes in the translome and the transcriptome. (A) Scatterplot of changes in ribosome footprint counts (Ribo-Seq) plotted against RNA abundance (RNA-Seq) in HEK293TΔYB-1 compared to HEK293T. Genes with significantly changed RNA abundance (multiple-testing corrected  $P$ -values < 0.05) are highlighted in red (upregulated) or blue (downregulated). (B) Volcano plot of ribosome occupancy changes in HEK293TΔYB-1 versus HEK293T; *YBX3* is highlighted in green. Genes with non-corrected  $P$ -value < 0.01 are labeled. (C) Gene set enrichment analysis (GSEA) of changes in RNA abundance (blue line) or ribosome occupancy (red line) in HEK293TΔYB-1 versus HEK293T. Vertical bars indicate the location of genes from a particular gene group in the sorted list.

First, using sucrose gradient centrifugation followed by qRT-PCR we confirmed the *YB-3* mRNA transition to polysomal fractions upon *YBX1* knockout (Fig. 3A). Next, in *YB-1*-null cells, we confirmed the increased *YB-3* amount by Western blotting (Fig. 3B). Of note, *YB-1* overexpression leads to a decreased *YB-3* level both in HEK293T and HEK293TΔYB-1. Thus, *YB-1* inhibits translation of *YB-3*. However, the abundance of *YB-3* mRNA changes in the opposite direction: it is decreased upon *YBX1* knockout and increased upon *YB-1* overexpression (Fig. 3C, qRT-PCR). Both observations agree with the high-throughput data. Importantly, the magnitude of the increased ribosome occupancy (1.25 log<sub>2</sub> fold change) considerably exceeds that of the decreased mRNA abundance (−0.64 log<sub>2</sub> fold change), as shown by Ribo-Seq and RNA-Seq data (Fig. 2A), thereby suggesting that the varying mRNA amount could be a secondary compensatory effect.

According to both high-throughput (RIP-Seq) and low-throughput (immunoprecipitation with *YB-1* antibodies followed by RT-PCR, Supplementary Fig. S6) data, *YB-3* mRNA is bound to *YB-1*. Thus, *YB-1* could directly regulate *YB-3* mRNA translation. We verified this in the cell-free translation system obtained from HEK293T cells using the reporter mRNA with 5' and 3' UTRs of the *YB-3* mRNA (Fig. 3D). Indeed, *YB-1* specifically inhibits translation of the *YB-3* reporter mRNA.

Thus, *YB-3* synthesis is controlled by *YB-1* at the mRNA abundance level, by affecting either transcription or stability, and at the mRNA translation level.

#### ***In HEK293TΔYB-1 cells, YB-3 substitutes YB-1 in mRNA binding***

*YB-1* and *YB-3* have homologous sequences and similar domain organization (Fig. 4A): they have almost identical

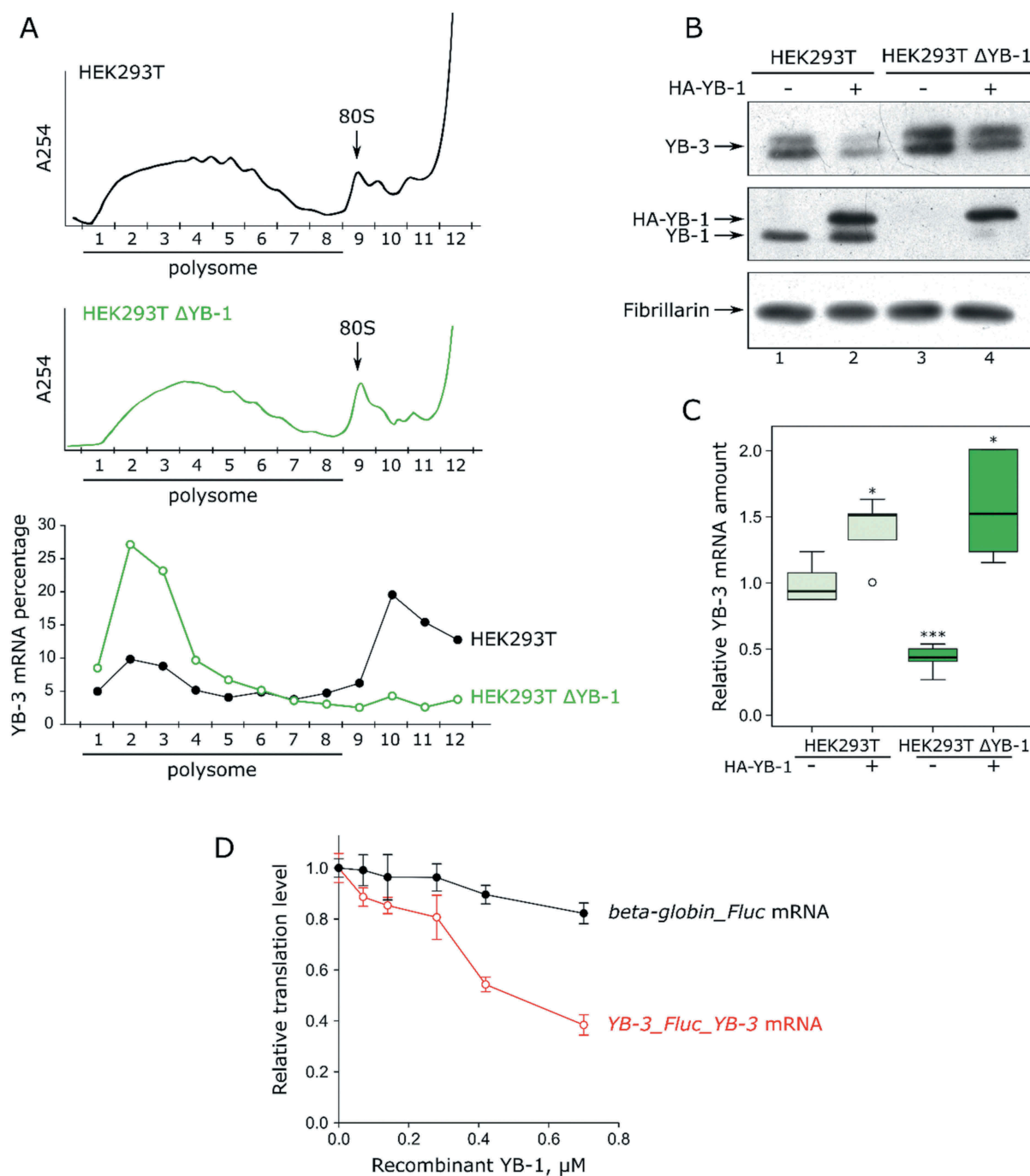


**Figure 3.** YB-1 controls YB-3 synthesis. (A) The lysates of HEK293T and HEK293T $\Delta$ YB-1 cells were subjected to centrifugation through 15–45% linear sucrose gradient for 1 h at 45,000 rpm in an SW-60 rotor. Profiles of optical density at A254 are shown (upper and middle panels). YB-3 mRNA was detected by qRT-PCR in each fraction of the polysome gradient (lower panel). (B) Changes in the amount of YB-1 in HEK293T cells upon knockout or plasmid-induced expression of YB-1 detected by Western blotting; Fibrillarin is given as a control. (C) Changes in the amount of YB-3 mRNA in HEK293T cells with knockout or overexpression of YB-1 detected by qRT-PCR. YB-3 mRNA amounts were normalized to those of HEK293T cells transfected by the empty vector. Two-tailed Student's t-test was used to estimate the statistical significance versus HEK293T cells transfected by the empty vector. \*\*\* $p < 0.001$ , \* $p < 0.05$ . (D) 0.15 pmol of capped and polyadenylated reporter *Firefly luciferase* mRNAs with indicated UTRs were translated in HEK293T cell-free translation extract in the presence of increasing concentrations of recombinant YB-1 (0, 0.07, 0.14, 0.28, 0.42, and 0.7  $\mu$ M). After 1 h incubation at 30°C, Fluc activity was measured. The values were normalized to the Fluc activity without the addition of YB-1. Values are the means of at least three independent replicates. Error bars show 2 standard deviations.

cold shock domains, disordered N- and C-termini with a similar amino acid composition, and a similar distribution of charged amino acid residues in the C-terminal domain [1,18]. The specific affinity of YB-1 is believed to be determined by the cold shock domain [19,20], and one can expect a similar set of YB-1- and YB-3-bound mRNAs.

We performed RIP-Seq with YB-3 antibodies in HEK293T and HEK293T $\Delta$ YB-1 cells. Indeed (Fig. 4B, Supplementary Fig. S7), YB-1 and YB-3 share a similar set of bound mRNAs. RIP-Seq of YB-3 detects about 80% of the transcribed RNAs, and the immunoprecipitation efficiencies of YB-1 and YB-3 are strongly positively correlated (Pearson's

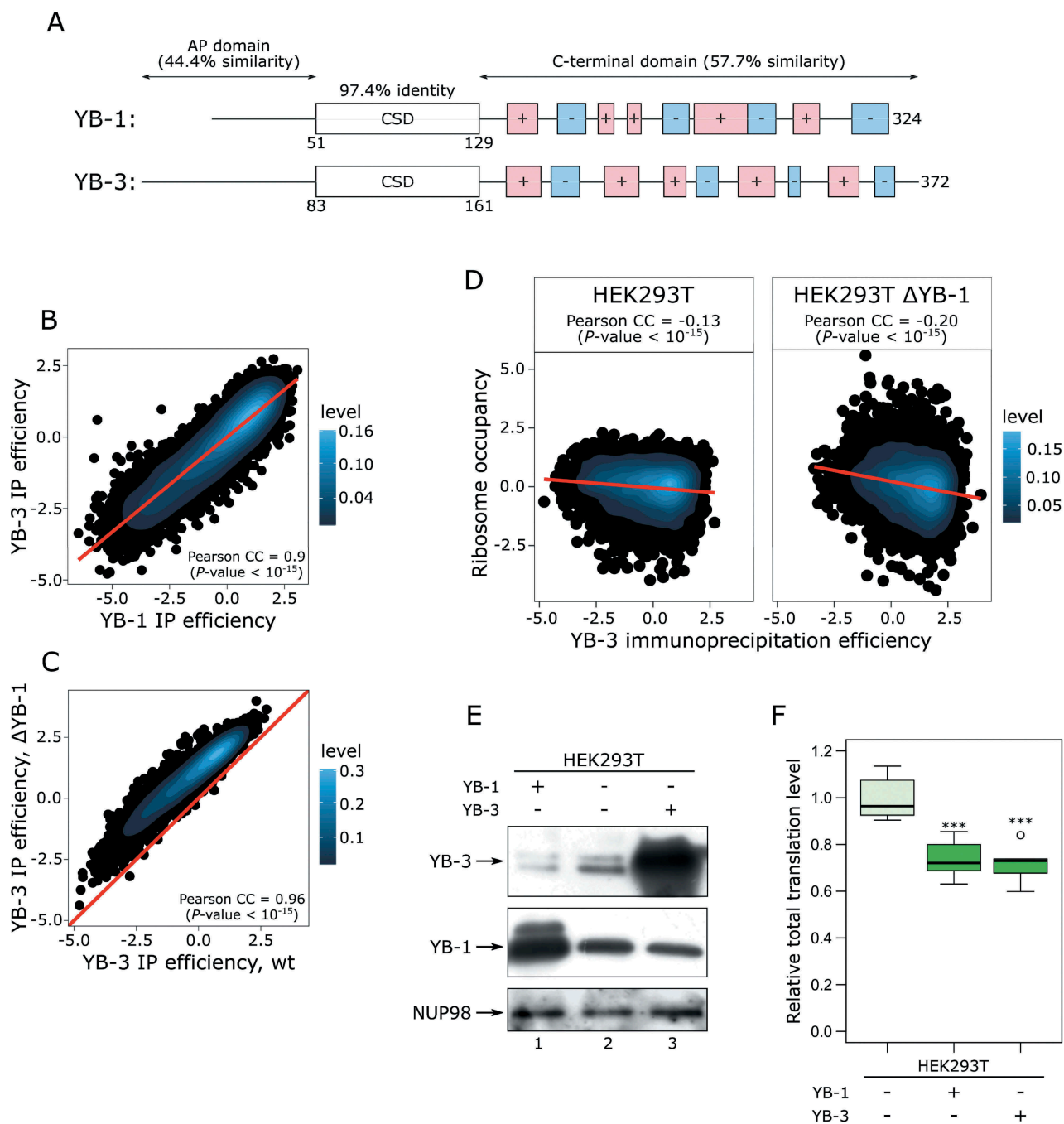


**Figure 4.** YB-3 replaces YB-1 on mRNAs of HEK293TΔYB-1 cells. (A) Domain organization of Y-box-binding proteins. Relative positions of clusters of positively- (red) and negatively charged (blue) amino acid residues are shown. AP-domain: alanine/proline-rich domain, CDS: cold shock domain. (B) Scatterplot of the YB-1 and YB-3 immunoprecipitation efficiency in HEK293T. The two-dimensional kernel density estimation, the linear regression line, the Pearson's correlation coefficient, and the significance of correlation ( $P$ -value) are shown. (C) Scatterplot of the YB-3 immunoprecipitation efficiency in HEK293T and HEK293TΔYB-1. The two-dimensional kernel density estimation, the Pearson's correlation coefficient, the significance of correlation ( $P$ -value), and the reference diagonal ( $y = x$ ) line are shown. To estimate absolute changes of the YB-3 immunoprecipitation efficiency upon *YBX1* knockout, the data were re-normalized to spike-ins. (D) Scatterplot of the ribosome occupancy ( $Y$ -axis) and the YB-3 immunoprecipitation efficiency in HEK293T (left) or HEK293TΔYB-1 (right). The two-dimensional kernel density estimation, the linear regression line, the Pearson's correlation coefficient, and the significance of correlation ( $P$ -value) are shown. For each gene, the ribosome occupancy (Ribo-Seq read counts normalized to the RNA-Seq read counts) was estimated at coding segments, excluding UTRs. (E) Changes in the YB-1 and YB-3 amount in HEK293T cells after the plasmid-induced overexpression of YB-1 or YB-3, as revealed by Western blotting. NUP98 was used as a loading control. (F) The total translation level of HEK293T cells transfected either by the empty vector pcDNA3.1-puro, or pcDNA3.1-puro-YB-1 (YB-1), or pcDNA3.1-puro-YB-3 (YB-3) assessed from the incorporation of azidohomoalanine. The values were computed as follows: for each biological replicate, the values were normalized to the mean value of a particular replicate; the obtained values were then normalized across experiments to the mean value detected for HEK293T cells transfected by the empty vector. Two-tailed Student's  $t$ -test was used to estimate the statistical significance versus HEK293T cells transfected by the empty vector. \*\*\* $p < 0.001$ .

CC = 0.9,  $P < 10^{-15}$ ). Furthermore (Fig. 4C), the YB-3 binding efficiency globally increases in HEK293TΔYB-1 cells versus wild type HEK293T.

These data suggest that YB-3 could serve as a partial substitute for YB-1. In the same way as for YB-1, we compared the ribosome occupancy of CDSs and the YB-3

immunoprecipitation efficiency of the whole transcripts (Fig. 4D), which showed the same pattern as for YB-1 (Fig. 1A). Interestingly, in HEK293T $\Delta$ YB-1, the negative correlation between the YB-3 immunoprecipitation efficiency and the ribosome occupancy was even stronger. Furthermore, we found a significant positive correlation when comparing YB-1 overexpression and *YBX1* knockout by considering RNA-Seq (Pearson's  $CC = 0.39$ ,  $P < 10^{-15}$ ), Ribo-Seq ( $CC = 0.35$ ,  $P < 10^{-15}$ ), or RO changes relative to HEK293T (Supplementary Fig. S8A). Of note, the correlation for changes in the ribosome occupancy was even higher (Pearson's  $CC = 0.59$ ,  $P < 10^{-15}$ ).

Taken together, YB-1-null cells have a similar molecular phenotype to that of YB-1-overexpressing cells, probably achieved through strong upregulation of YB-3. In turn, YB-3 overexpression could be the cause of the global translation decrease in HEK293T $\Delta$ YB-1. Further, we measured the global translation level in YB-3- or YB-1-overexpressing cells (Fig. 4E,F). In both cases, global protein synthesis was reduced by approximately 25% in comparison to HEK293T cells. Thus, YB-3, like YB-1, is a global translation inhibitor and functionally substitutes YB-1 in HEK293T $\Delta$ YB-1.

## Discussion

YB-1 is a DNA- and RNA-binding protein that participates in multiple DNA- and RNA-dependent processes, including regulation of RNA transcription, translation, and stability [1]. Although YB-1 involvement in transcription regulation is widely studied, it remains unclear [2,4]. First, YB-1 is a predominantly cytoplasmic protein that goes to the nucleus only in specific conditions, such as inhibited transcription and DNA-damaging stress [21–25]. Second, according to ChIP-Seq data, YB-1-bound DNA regions exhibit no clear sequence motif, which could be expected for transcription factors that specifically recognize DNA sites [4]. Our data also support the idea that YB-1 impact on transcription is of limited magnitude. In particular, we have detected no differentially expressed genes (passing 5% FDR) upon YB-1 overexpression (Supplementary Table S2). In HEK293T, we found a weak but significant positive correlation between the YB-1 immunoprecipitation efficiency and changes in RNA-Seq upon YB-1 overexpression (Supplementary Fig. S8B, Pearson's  $CC = 0.23$ ,  $P < 10^{-15}$ ). This correlation between overexpression-induced changes in RNA abundance and IP efficiency in wild type cells suggests that YB-1 could control RNA stability but not RNA transcription *per se*. This assumption is in agreement with the previous observations [5] reporting that YB-1 could package and stabilize RNAs in the form of untranslated mRNPs.

Y-box binding proteins of different organisms were initially recognized as the major mRNP proteins that pack and protect mRNAs [26,27]. Later, several mRNAs specifically binding to YB-1 were identified (see references in [1]). Since then, the degree of YB-1 RNA-binding specificity and the range of its mRNA targets in the cell were under debate. Previous studies found only 15–20% of all mRNAs to be bound by YB-1 [28,29]. However, more recent data, such as iCLIP in glioblastoma cells [30], reveal YB-1-binding sites in

RNAs of nearly 15 thousand genes, which is comparable to the mRNA diversity of the whole transcriptome. Of note, specific YB-1 binding sites were found only in 17% of the binding regions [30], thus suggesting that there was a major component of non-specific binding. In this study, using two different antibodies, we confirm that YB-1 binds about 80% of the transcriptome, and show that a similarly wide range of RNAs can be bound by YB-3. Taking into account the strong positive correlation between RIP-Seq and RNA-Seq in wild-type HEK293T (Supplementary Fig. S1A), we consider that Y-box-binding proteins bind the majority of RNAs in a non-specific way, probably involving indirect interactions facilitated by other RNA-binding proteins.

YB-1 plays a dual role in mRNA translation. At a high YB-1-to-RNA ratio, YB-1 inhibits translation either by competing with eIF4F and PABP [6,31] and by packaging mRNA into free mRNPs [9,32]. At a low YB-1-to-RNA ratio, YB-1 stimulates translation probably by shifting translation initiation factors towards the 5'UTR [9,33] or unwinding the RNA secondary structure [34]. In this study, we found that a negative correlation between the ribosome occupancy and the YB-1 immunoprecipitation efficiency was becoming much more prominent upon YB-1 overexpression (Fig. 1A), in agreement with the decreased total translation level (Figs. 1D and 4F). Thus, in HEK293T cells, for the majority of the transcripts, YB-1 serves as a translation inhibitor.

In knockout cells, we expected the increased translation level for mRNAs with a high YB-1 binding efficiency and the decreased one for other transcripts. However, we observed the opposite effect, similar to that of YB-1-overexpressing cells (Supplementary Fig. S8C), i.e. the negative correlation between the YB-1 binding efficiency and the differential ribosome occupancy. This apparent contradiction can be explained as follows. Our data suggest that YB-3 is a partial functional substitute for YB-1. It is known that YB-3, along with YB-2 (another homolog of YB-1), is required for translation repression of hundreds of mRNAs in mouse testis [35]. However, YB-2 expression is limited to early development [36,37], and in HEK293T cells YB-2 is not expressed. As to YB-3, nothing was previously known about its involvement in the regulation of translation in somatic cells. Here we report that YB-3 is specifically overexpressed in YB-1-null cells. The increased amount of YB-3 can be the cause of the translation inhibition of YB-1 targets, which instead may be bound by YB-3.

The concept of functional interchangeability of YB-1 and YB-3 is supported by the following. First, YB-1 and YB-3 share similar cold shock domains (CSD), as well as structurally similar N- and C-termini [1]. For both YB-1 and YB-3, the AKT and RSK kinases phosphorylate the CSD at the same amino acid (Ser102 for YB-1 and Ser134 for YB-3) [38]. The CSDs of Y-box-binding proteins are believed to be responsible for specific RNA binding [19,20], suggesting that YB-1 and YB-3 bind similar sets of mRNAs. This study shows that this is indeed the case, the YB-3 mRNA binding is more exhibited in the absence of YB-1. Second, the previous YB-1- and YB-3-knockout experiments also indirectly demonstrated their partial functional interchangeability [8,17]. YB-3-null mice showed no other pathologies but

the lack of fertility, while double mutant embryos (YB-1<sup>-/-</sup> and YB-3<sup>-/-</sup>) had serious malformations and died sooner (8.5–11.5 days) than YB-1<sup>-/-</sup> embryos (13.5 days and perinatal death). Thus, YB-3 seems to functionally replace YB-1 at the early stages of embryo development, although later stages require precise functions of YB-1 that are not fully performed by the paralog.

Among numerous functions of YB-1, there are those specific to YB-1 only and not fulfilled by YB-3. In particular, a comparative GSEA analysis of changes in RNA-Seq and RO of HEK293TΔYB-1 versus wild-type HEK293T revealed a decreased RNA amount but an increased ribosome occupancy of mRNAs related to the cell cycle and cellular respiration. It was shown previously that YB-1 selectively interacts with and suppresses translation of mRNAs coding for cyclins, growth factors, and translation factors [29]. Also, YB-1 acts as a negative regulator of translation of mitochondrial oxidative phosphorylation (OXPHOS) mRNAs [39]. Thus, we hypothesize that YB-1 binds and stabilizes these mRNAs and specifically inhibits their translation.

A very different case is represented by mRNAs related to TGF-β signaling. Upon *YBX1* knockout, for these transcripts, both the mRNA amount and, to a lower extent, the ribosome occupancy were increased. Probably, for these mRNAs, the YB-1 influence is limited to translational control, but YB-3 cannot fully compensate for its loss. This is of special interest since YB-1 is known to somewhat act as an antagonist in TGF-β signaling [13,14]; also, YB-1 and TGF-β counter-regulate each other [15,16]. Besides, activation of the TGF-β signaling cascade is associated with a slowdown of cell division [40], which agrees with a reduced rate of HEK293TΔYB-1 cell division.

Another important example of specific translational control by YB-1 is the translation repression of *YB-3* mRNA. In the YB-1-null cells, the YB-3 level is increased due to strongly enhanced mRNA translation, whereas in normal conditions and upon YB-1 overexpression *YB-3* mRNA is translated at a very low level. The molecular mechanism of this translational control is obscure. It is known that YB-1 negatively regulates translation of its own mRNA through a regulatory element within the 3'UTR [41,42]. Probably, in the case of *YB-3* mRNA, the translation inhibition also involves YB-1 binding to specific sites in the untranslated regions. In particular, we observed YB-1-induced inhibition of translation of the reporter mRNA carrying 5' and 3' UTRs of the *YB-3* mRNA (Fig. 3D).

Interestingly, the cross-regulation, although at the splicing level, was previously reported for pairs of other homologous RNA-binding proteins [43], such as hnRNPD and D-like protein [44]. Regarding Y-box binding proteins and translational control, the ability of YB-3 to inhibit *YB-1* or *YB-3* mRNA translation is still questionable.

All in all, for Y-box-binding proteins, further analysis of the post-transcriptional regulatory loop and its possible cell-type specificity is required to fully describe their regulatory functions.

## Methods

### Plasmids

pSpCas9(BB)-2A-Puro (a gift from Feng Zhang; Addgene plasmid #48,139) [45], pcDNA3-HA-YB-1 and pcDNA3-HA [5], pGFP-c3 [46], pNL2.2 SLU7-NlucP [47], pSP36TLuc-A50 [48], pcDNA-3.1-puro (kindly provided by Dr. Dmitriev, A.N. Belozersky Institute of Physico-Chemical Biology, MSU).

pcDNA-3.1-puro-YB-1, pcDNA-3.1-puro-YB-3, pSP36T-5' UTR YB-3-FLuc-3'UTR YB-3-A50 (the plasmids cloning described in the Supplementary Text).

### Antibodies

Polyclonal rabbit antibody against YB-1 (4202, Cell Signaling), polyclonal rabbit antibody against YB-1 (A303-230A, Bethyl), polyclonal rabbit antibody against YB-3 (A303-070A, Bethyl), monoclonal rabbit antibody against Fibrillarin (2639, Cell Signaling), monoclonal rabbit antibody against NUP98 (2598, Cell Signaling), anti-rabbit HRP-conjugated antibody (7074, Cell Signaling).

### Cell cultures

HEK293T cells (originally obtained from ATCC) were kindly provided by Dr. Elena Nadezhdina (Institute of Protein Research, RAS). The cells were cultivated in Dulbecco's Modified Eagle's Medium (DMEM) supplemented with 10% fetal calf serum, 2 mM glutamine, 100 U/ml penicillin, and 100 µg/ml streptomycin. The cells were incubated at 37°C in a humidified atmosphere containing 5% CO<sub>2</sub> and passaged by standard methods.

The number of cells in experiments was determined using a Countess automated cell counter (Invitrogen).

For DNA transfection experiments, the cells were cultured on a 6-well plate to a density of 80–90%. The cells were transfected using Lipofectamine 3000 (Invitrogen). For transfection, 5 µg of the plasmid mixture (1 µg of pcDNA3-HA-YB-1 and 4 µg of pcDNA3-HA or 5 µg of pcDNA3-HA only) was incubated with 10 µl of the P3000 reagent and 7.5 µl of the Lipofectamine 3000 in 250 µl Opti-MEM for 5 min and then added to the growth medium. 12 hours later, the cells were plated onto a new 100-mm dish and cultivated for 36 h. To obtain YB-1- and YB-3-overexpressing cells (Fig. 4E,F), 5 µg of pcDNA-3.1-puro, or pcDNA-3.1-puro-YB-1, or pcDNA-3.1-puro-YB-3 was used in DNA transfection experiments.

### Western blotting

The cultured cells were washed with phosphate-buffered saline and lysed in the SDS-electrophoresis sample buffer. Proteins were separated by SDS-PAGE and transferred onto a nitrocellulose membrane. The membrane was blocked for 1 h at room temperature with non-fat 5% milk in TBS (10 mM Tris-HCl, pH 7.6, and 150 mM NaCl) and incubated overnight at 4°C in TBS-T (10 mM Tris-HCl, pH 7.6, 150 mM

NaCl, 0.05% Tween 20) supplemented with BSA (5%) and appropriate antibodies. The membrane was washed three times with TBS-T, incubated for 1 h with 5% non-fat milk in TBS-T and secondary antibodies conjugated with horseradish peroxidase, and then washed three times with TBS-T. Immunocomplexes were detected using an ECL Prime kit (GE Healthcare) according to the manufacturer's recommendations.

### **YBX1 knockout using a CRISPR/Cas9 genome editing system**

gRNAs targeting the first exon of YB-1 were designed using CRISPR Design software from the Zhang lab (crispr.mit.edu). Oligonucleotides were annealed and cloned into pSpCas9 (BB)-2A-Puro according to [45]. gRNAs target the sequences 5'-ACACCAAGCCCGCACTACG-3' within the YB-1 first exon: pSpCas9(BB)-2A-Puro plasmid with cloned gRNAs were transfected into HEK293T cells using Lipofectamine 3000 (Invitrogen). After puromycin treatment (1 µg/ml) for three days, the cells were allowed to recover for two days and then the pool of survived cells were cloned by limiting dilution and screened by Western blotting.

### **Genotyping of YBX1**

Genome DNA of HEK293TΔYB-1 cells was obtained using The Genomic DNA Purification Kit (Thermo Fisher Scientific) according to the manufacturer's recommendations. For genotyping, a *YBX1* fragment was amplified by polymerase chain reaction (PCR) using primers located within the first exon and first intron of *YBX1* gene (Forward: 5'-CAGTCACCATCACCGCAACCATG-3', Reverse: 5'-AGCTCCGGCTAACGGTTCCTCGCT-3') using Pfu polymerase (Thermo Fisher Scientific). Amplicons were cloned into pJet1.2 (Thermo Fisher Scientific) and sequenced individually (Evrogen).

### **Measuring the total translation level per cell**

The total translation level per cell was determined from the incorporation of azidohomoalanine in newly synthesized proteins, followed by its crosslinking with an alkyne derivative of the fluorescent dye Alexa Fluor 488 [49]. The cells were cultured on a 6-well plate to a density of 60-70%. Then DMEM was replaced by methionine-free DMEM, and the cells were incubated in the absence of FBS for 45 min under standard conditions. Then the reaction mixture was replaced by fresh methionine-free DMEM containing azidohomoalanine (50 µM). After 2 h incubation, the cells were washed with ice-cold PBS, and 200 µl of lysis buffer (1% SDS in 50 mM Tris-HCl (pH 8.0) and Benzonase (250 U/ml)) was added to each well of the plate. A 200 µg sample of lysate was diluted with water to a volume of 77 µl and mixed with 100 µl of alkyne-containing PBS buffer. Then the mixture was supplemented with 3 µl of freshly prepared CuSO<sub>4</sub>-THPTA (Tris (3-hydroxypropyltriazolyl-methyl)amine) mix (1 µl CuSO<sub>4</sub> (20 mM) and 2 µl THPTA (50 mM)), 10 µl aminoguanidine (100 mM), and 10 µl of freshly prepared sodium ascorbate

(100 mM) and incubated at room temperature for 1 h in the dark. After incubation, the reaction mixture was supplemented with 600 µl methanol, 150 µl chloroform, and 400 µl water, well-mixed and subjected to centrifugation at 13,000 g for 5 min. Then the aqueous phase was removed and replaced by 450 µl methanol, and centrifugation at 13,000 g was continued for 5 min. The methanol washing was repeated twice, after which the pellet was let dry for 1 h and then dissolved in 200 µl of 1.5x sample buffer for SDS-PAGE.

For all samples, equal total protein amounts were separated by SDS-PAGE and Alexa Fluor 488-labeled proteins were detected on a ChemiDoc MP Imaging System (Bio-Rad) and processed using the OptiQuant Software (Packard Instruments). To estimate the translation level per cell, equal numbers of cells were lysed in the SDS-electrophoresis sample buffer and separated by SDS-PAGE. The total protein amount was estimated by Coomassie blue staining using OptiQuant Software. The total translation level per cell was estimated as the Alexa Fluor 488 fluorescence normalized to the total protein amount per cell.

### **Analysis of mRNA distribution between polysomes and free mRNPs**

Cells were washed twice with ice-cold PBS containing 0.1 mg/ml cycloheximide and lysed directly on the plate after addition of 400 µl of polysome extraction buffer: 15 mM Hepes-KOH, pH 7.6, 5 mM MgCl<sub>2</sub>, 0.3 M NaCl, 1% Triton X-100, 0.1 mg/ml cycloheximide, and 0.2 mM VRC (vanadylribonucleoside complex), 1 mM DTT. Extracts were transferred into 1.5 ml tubes and incubated on ice for 10 min with occasional mixing. The nuclei and debris were removed by centrifugation at 12,000 g for 10 min in a microcentrifuge. 45 µl aliquots of supernatants were layered onto 4.5 ml of 15-45% sucrose gradient in buffer (15 mM Hepes-KOH, pH 7.6, 5 mM MgCl<sub>2</sub>, 100 mM KCl, 0.1 mM EDTA, and 0.01 mg/ml cycloheximide) and centrifuged in a SW-60 rotor (Beckman Coulter) at 45,000 rpm for 55 min at 4°C. All gradients were monitored for absorbance at 254 nm during their collection from the bottom. 0.375 ml fractions were collected and 0.1 ng of *in vitro* transcribed *Nanoluc luciferase* (*Nluc*) mRNA was added to each fraction for normalization.

### **Quantitative reverse transcription PCR (qRT-PCR)**

Total RNA was obtained from cells or sucrose gradient fractions using TRIzol LS Reagent (Thermo Fisher Scientific) according to the manufacturer's recommendations. Up to 1 µg of total RNA was used in reverse transcription reaction with Maxima H Minus Reverse Transcriptase (Thermo Fisher Scientific). Quantitative real-time PCR (qRT-PCR) was performed on a DTLite Real-Time PCR System (DNA Technology) using qPCRMix-HS SYBR+LowROX reaction mixture (Evrogen). A 25 µl aliquot of final reaction mixture contained 1/40 of the RT reaction mixture and 0.4 µM primers (see Supplementary Table S1). The following cycling conditions were used: 5 min at 95°C followed by 50 cycles of 95°C for 10 sec, 59°C for 20 sec and 72°C for 10 sec. For the

total RNA samples, the statistical data analysis and assessment of differences in gene expression were performed using the REST2009 software; the reference genes were *BTF3* and *ALDH16A*. For sucrose gradient fractions, transcript abundance values were normalized to those of *Nluc* mRNA.

### Transcription *in vitro*

RNA was transcribed by T7 RNA polymerase using a HiScribe T7 High Yield RNA Synthesis Kit (NEB). Spike-in *Fluc* RNA was transcribed from FLuc Control Template (NEB), spike-in *GFP* RNA was transcribed from pGFP-c3 linearized with *EcoRI*. DNA template for *Nluc* mRNA was obtained by PCR amplification of the pNL2.2 SLU7-NlucP with the primers (Forward 5'-TAATACGACTCACTATAGGGATTACGAGATTGGCTTG-GATTC-3' and Reverse 5'-TGTGTGTTAACTTGTATTGCA GCTTATAATG-3', T7-promoter is underlined). RNAs were polyadenylated using the A-Plus Poly(A) Polymerase Tailing Kit (CellScript) according to the manufacturer's manual.

Reporter mRNAs for *in vitro* translation experiments were transcribed with a SP6-Scribe Standard RNA IVT Kit (CellScript). Polyadenylated *YB-3\_Fluc\_YB-3* mRNA was transcribed from pSP36T-5'UTR\_YB-3-FLuc-3'UTR\_YB-3-A50 linearized with *HpaI*. Polyadenylated *beta-globin\_Fluc* mRNA was transcribed from pSP36TLuc-A50 linearized with *SmaI*. mRNAs were capped using the ScriptCap m<sup>7</sup>G Capping System and the ScriptCap 2'-O-Methyltransferase Enzyme (CellScript) according to the manufacturer's manual.

### *In vitro* translation

HEK293T cell extract for the cell-free translation system was obtained as described previously [50]. Recombinant YB-1 was purified as described previously [51].

The translation mixture (10  $\mu$ l) consisted of 5  $\mu$ l HEK293T cell extract, 1  $\mu$ l 10X translation buffer (200 mM Hepes-KOH, pH 7.6, 10 mM DTT, 5 mM spermidine-HCl, 80 mM creatine phosphate, 10 mM ATP, 2 mM GTP, and 250  $\mu$ M of each amino acid), 100 mM KAc, 1 mM Mg(Ac)<sub>2</sub>, 2 units of Human Placental Ribonuclease Inhibitor (Fermentas), 0.15 pmol reporter *Fluc* mRNA, and recombinant YB-1 protein. Reaction mixtures were incubated for 1 h at 30°C, and then the luciferase activities were measured using the OneGlo Luciferase Assay kit (Promega).

### Ribosome profiling

Ribosome profiling was performed using the TruSeqRibo Profile kit (Illumina) with modifications described below. HEK293T, HEK293T $\Delta$ YB-1, and HEK293T overexpressing HA-YB-1 cells at 70-80% confluency were immediately chilled on ice and washed with PBS + cycloheximide (100  $\mu$ g/ml). The cells were not pre-treated with cycloheximide to avoid the artificial accumulation of initiation complexes at translation initiation starts [52]. The cells were then lysed with buffer containing 20 mM Tris-HCl (pH 7.4), 150 mM NaCl, 5 mM MgCl<sub>2</sub>, 1 mM DTT, 1% Triton X-100, 100  $\mu$ g/ml cycloheximide (Sigma-Aldrich), 25 U/ml TURBO DNase (Ambion). Cell lysates were incubated on ice for

10 min, triturated ten times through a 26-G needle and centrifuged at 20,000 *g* at +4°C for 10 min. The supernatant was divided into two parts: for Ribo-Seq and size-matched RNA-Seq library preparation. Nuclease footprinting and ribosome recovery for Ribo-Seq library preparation were performed according to [53]. Total RNA for RNA-Seq library preparation was isolated using TRIzol LS Reagent (Thermo Fisher Scientific).

Subsequent procedures were performed using a TruSeqRibo Profile Kit (Illumina) according to the manufacturer's protocol. rRNA depletion was performed using a Ribo-Zero rRNA Removal Kit (Human/Mouse/Rat) (Illumina) according to the manufacturer's recommendations.

### RNA immunoprecipitation and sequencing (RIP-Seq)

RNA immunoprecipitation was performed as described by Tenenbaum et al., [54] with some modifications. Briefly, cells were washed twice with ice-cold PBS and removed from culture plates with a scraper. Then cells were resuspended in approximately two pellet volumes of lysis buffer containing 10 mM Hepes-KOH, pH 7.0, 100 mM KCl, 5 mM MgCl<sub>2</sub>, 0.5% Nonidet P-40 with 1 mM DTT, 100 U/ml RNase Inhibitor (Thermo Fisher Scientific), 0.2% vanadylribonucleoside complex (Fluka), and Protein Inhibitor Cocktail (Roche) added fresh at the time of use. The lysed cells were then frozen and stored at -80°C. At the time of use, the cell lysate was thawed and centrifuged at 16,000 *g* in a microfuge for 10 min at 4°C. For immunoprecipitation, Protein G Sepharose beads (GE Healthcare) were swollen 1:5 V/V in NT2 Buffer (50 mM Tris-HCl, pH 7.6, 150 mM NaCl, 1 mM MgCl<sub>2</sub>, 0.05% Nonidet P-40) supplemented with 5% BSA. A 300  $\mu$ l aliquot of the 1:5 V/V pre-swollen protein G bead slurry was used per immunoprecipitation reaction and incubated overnight at 4°C with an excess of YB-1 or YB-3 antibody (5--10  $\mu$ g). The antibody-coated beads were washed with ice-cold NT2 buffer and resuspended in 900  $\mu$ l of NT2 buffer supplemented with 100 U/ml RNase Inhibitor, 0.2% vanadylribonucleoside complex, 1 mM DTT, 20 mM EDTA. The beads were briefly vortexed, and 100  $\mu$ l of cell lysate was added and immediately centrifuged, and a 100  $\mu$ l aliquot removed to represent total cellular RNA. The immunoprecipitation reactions were performed at room temperature for 2 h and then beads were washed 4 times with ice-cold NT2 buffer followed by 2 washes with NT2 buffer supplemented with 1 M urea. Washed beads were resuspended in 100  $\mu$ l NT2 buffer. Immunoprecipitated and total RNA were isolated using TRIzol LS Reagent according to the manufacturer's protocol.

Libraries for sequencing were obtained using a NEBNext Ultra Directional RNA Library Prep Kit for Illumina (NEB) according to the manufacturer's protocol. rRNA depletion was performed using a NEBNext Poly(A) mRNA Magnetic Isolation Module (NEB) or a NEBNext rRNA Depletion Kit (Human/Mouse/Rat) (NEB) according to the manufacturer's protocol.

For selected samples (polyA RIP-Seq YB-3 and polyA RNA-Seq in HEK293T and HEK293T $\Delta$ YB-1) spike-ins (7 pg GFP mRNA and 0.12 pg FLuc mRNA) were added per 0.5  $\mu$ g of RNA at the start of library preparation.

## High-throughput sequencing and data processing

Libraries were sequenced on Illumina HiSeq 2000 (Laboratory of Evolutionary Genomics, FBB MSU) and Illumina NextSeq 500 (Skoltech Genomics Core Facility).

Reads quality control was performed with FastQC v0.11.5 (<http://www.bioinformatics.babraham.ac.uk/projects/fastqc>). Overview of samples, sequencing, and read mapping statistics are presented in Supplementary Table S2. The reads were processed as follows: trimming was performed with cutadapt v1.18 [55] to remove adapter sequences; mapping to the hg38 genome assembly [56] with GENCODE v29 genome annotation [57] was performed with STAR v2.6.1d [58], which also provided gene counts for the whole transcripts. Reads counts for coding segments (used in Figs. 1A and 4D, Supplementary Fig. S1B for CDS-level ribosome occupancy estimates, see below) were obtained with plastid v.0.4.8 [59].

For samples with spike-ins, the respective sequences were added to the genome assembly as separate chromosomes. Across samples, from 10 to 99 million reads passed trimming (median of 38 million), 9 to 31 million (median of 17 million) reads were uniquely mapped. Resulting read counts from several sequencing runs of the same sample were summed up. The principal component analysis of samples shows a reasonable separation of experiment types and agreement between replicates (Supplementary Fig. S9A).

Ribo-Seq data have clear triplet periodicity, metagene profiles of windows surrounding gene start codons were obtained with plastid v.0.4.8 [59] and visualized in Supplementary Fig. S9B.

The differential gene expression and gene set enrichment analyses were performed in the R environment. Gene counts for rRNA and mt-rRNA were excluded. Genes passing 1 count-per-million in all samples were used in further analysis. Read counts per gene were normalized with the edgeR TMM method [60]. Additionally, polyA YB-3 RIP-Seq in HEK293TΔYB-1 was re-normalized to that of HEK293T using spike-ins (mean estimate for two spike-ins), the same was performed for polyA RNA-Seq. Spike-in normalization allowed to estimate absolute changes in the YB-3 immunoprecipitation efficiency upon *YBX1* knockout.

Samples of (HEK293T and HEK293T+HA) or (HEK293TΔYB-1 and HEK293TΔYB-1+HA) showed similar expression patterns and were used as replicates. Differential gene expression (changes in RNA-Seq and Ribo-Seq), ribosome occupancy (Ribo-Seq relative to size-matched RNA-Seq, RO values for particular cell types, and differential ribosome occupancy between cell types), and immunoprecipitation (IP) efficiency (RIP-Seq relative to standard RNA-Seq) were estimated using contrasts of the edgeR generalized linear model (glmQLFit, glmQLFTest). *P*-values were corrected for multiple testing using FDR (Benjamini-Hochberg). CDS read counts were used for ribosome occupancy estimates in Figs. 1A and 4D, Supplementary Fig. S1B; whole-transcript read counts were used elsewhere.

The Gene Set Enrichment Analysis (GSEA) was performed using a *fgsea* bioconductor package [61]. GO terms were obtained from MSIGdb v6.2 [62]. Gene ranking was obtained using the signed *P*-value (sign taken from the fold change, more significant up- and down-

regulated genes appear at the top and bottom of the list, respectively).

## Acknowledgments

We thank Maria Logacheva (Skoltech Genomics Core Facility) and Alexey Penin (Laboratory of Evolutionary Genomics, FBB MSU) for their invaluable assistance with high-throughput sequencing. We thank E. Serebrova for help in manuscript preparation.

## Disclosure statement

No potential conflict of interest was reported by the authors.

## Funding

This work was supported by the Russian Science Foundation (#19-74-20129) [high-throughput sequencing experiments] and the Russian Foundation for Basic Research (#18-04-00595) [section 'YB-1 controls YB-3 expression']. Open access is funded by the Russian Science Foundation (#19-74-20129)

## Data access

The data are deposited to the NCBI GEO under accession number GSE130781.

## ORCID

D. N. Lyabin  <http://orcid.org/0000-0003-4605-8884>

## References

- Eliseeva IA, Kim ER, Guryanov SG, et al. Y-box-binding protein 1 (YB-1) and its functions. *Biochemistry (Mosc)*. 2011;76:1402–1433.
- Lyabin DN, Eliseeva IA, Ovchinnikov LP. YB-1 protein: functions and regulation. *Wiley Interdiscip Rev RNA*. 2014;5:95–110.
- Shurtleff MJ, Temoche-Diaz MM, Karfilis KV, et al. Y-box protein 1 is required to sort microRNAs into exosomes in cells and in a cell-free reaction. *eLife*. 2016;5.
- Dolfini D, Mantovani R. YB-1 (YBX1) does not bind to Y/CCAAT boxes in vivo. *Oncogene*. 2013;32:4189–4190.
- Evdokimova V, Ruzanov P, Imataka H, et al. The major mRNA-associated protein YB-1 is a potent 5' cap-dependent mRNA stabilizer. *Embo J*. 2001;20:5491–5502.
- Nekrasov MP, Ivshina MP, Chernov KG, et al. The mRNA-binding protein YB-1 (p50) prevents association of the eukaryotic initiation factor eIF4G with mRNA and inhibits protein synthesis at the initiation stage. *J Biol Chem*. 2003;278:13936–13943.
- Evdokimova V, Tognon C, Ng T, et al. Translational activation of *snail1* and other developmentally regulated transcription factors by YB-1 promotes an epithelial-mesenchymal transition. *Cancer Cell*. 2009;15:402–415.
- Lu ZH, Books JT, Ley TJ. YB-1 is important for late-stage embryonic development, optimal cellular stress responses, and the prevention of premature senescence. *Mol Cell Biol*. 2005;25:4625–4637.
- Minich WB, Ovchinnikov LP. Role of cytoplasmic mRNP proteins in translation. *Biochimie*. 1992;74:477–483.
- Basaki Y, Taguchi K, Izumi H, et al. Y-box binding protein-1 (YB-1) promotes cell cycle progression through CDC6-dependent pathway in human cancer cells. *Eur J Cancer*. 2010;46:954–965.

- [11] En-Nia A, Yilmaz E, Klinge U, et al. Transcription factor YB-1 mediates DNA polymerase alpha gene expression. *J Biol Chem.* 2005;280:7702–7711.
- [12] Evdokimova VM, Kovrigina EA, Nashchekin DV, et al. The major core protein of messenger ribonucleoprotein particles (p50) promotes initiation of protein biosynthesis in vitro. *J Biol Chem.* 1998;273:3574–3581.
- [13] Dooley S, Said HM, Gressner AM, et al. Y-box protein-1 is the crucial mediator of antifibrotic interferon-gamma effects. *J Biol Chem.* 2006;281:1784–1795.
- [14] Lindquist JA, Mertens PR. Cold shock proteins: from cellular mechanisms to pathophysiology and disease. *Cell Commun Signal.* 2018;16:63.
- [15] Fraser DJ, Phillips AO, Zhang X, et al. Y-box protein-1 controls transforming growth factor-beta1 translation in proximal tubular cells. *Kidney Int.* 2008;73:724–732.
- [16] Kato M, Wang L, Putta S, et al. Post-transcriptional up-regulation of Tsc-22 by Ybx1, a target of miR-216a, mediates TGF- $\beta$ -induced collagen expression in kidney cells. *J Biol Chem.* 2010;285:34004–34015.
- [17] Lu ZH, Books JT, Ley TJ. Cold shock domain family members YB-1 and MSY4 share essential functions during murine embryogenesis. *Mol Cell Biol.* 2006;26:8410–8417.
- [18] Kleene KC. Y-box proteins combine versatile cold shock domains and arginine-rich motifs (ARMS) for pleiotropic functions in RNA biology. *Biochem J.* 2018;475:2769–2784.
- [19] Bouvet P, Matsumoto K, Wolffe AP. Sequence-specific RNA recognition by the *Xenopus* Y-box proteins. An essential role for the cold shock domain. *J Biol Chem.* 1995;270:28297–28303.
- [20] Yang XJ, Zhu H, Mu SR, et al. Crystal structure of a Y-box binding protein 1 (YB-1)-RNA complex reveals key features and residues interacting with RNA. *J Biol Chem.* 2019;294:10998–11010.
- [21] Asakuno K, Kohno K, Uchiyama T, et al. Involvement of a DNA binding protein, MDR-NF1/YB-1, in human MDR1 gene expression by actinomycin D. *Biochem Biophys Res Commun.* 1994;199:1428–1435.
- [22] Fujita T, Ito K, Izumi H, et al. Increased nuclear localization of transcription factor Y-box binding protein 1 accompanied by up-regulation of P-glycoprotein in breast cancer pretreated with paclitaxel. *Clin Cancer Res.* 2005;11:8837–8844.
- [23] Koike K, Uchiyama T, Ohga T, et al. Nuclear translocation of the Y-box binding protein by ultraviolet irradiation. *FEBS Lett.* 1997;417:390–394.
- [24] Stein U, Jurchott K, Walther W, et al. Hyperthermia-induced nuclear translocation of transcription factor YB-1 leads to enhanced expression of multidrug resistance-related ABC transporters. *J Biol Chem.* 2001;276:28562–28569.
- [25] Tanaka T, Ohashi S, Saito H, et al. Indirubin 3'-oxime inhibits anticancer agent-induced YB-1 nuclear translocation in HepG2 human hepatocellular carcinoma cells. *Biochem Biophys Res Commun.* 2018;496:7–11.
- [26] Evdokimova VM, Wei CL, Sitikov AS, et al. The major protein of messenger ribonucleoprotein particles in somatic cells is a member of the Y-box binding transcription factor family. *J Biol Chem.* 1995;270:3186–3192.
- [27] Murray MT, Schiller DL, Franke WW. Sequence analysis of cytoplasmic mRNA-binding proteins of *Xenopus* oocytes identifies a family of RNA-binding proteins. *Proc Natl Acad Sci U S A.* 1992;89:11–15.
- [28] Dong J, Akcakanat A, Stivers DN, et al. RNA-binding specificity of Y-box protein 1. *RNA Biol.* 2009;6:59–64.
- [29] Evdokimova V, Ruzanov P, Anglesio MS, et al. Akt-mediated YB-1 phosphorylation activates translation of silent mRNA species. *Mol Cell Biol.* 2006;26:277–292.
- [30] Wu SL, Fu X, Huang J, et al. Genome-wide analysis of YB-1-RNA interactions reveals a novel role of YB-1 in miRNA processing in glioblastoma multiforme. *Nucleic Acids Res.* 2015;43:8516–8528.
- [31] Svitkin YV, Evdokimova VM, Brasey A, et al. General RNA-binding proteins have a function in poly(A)-binding protein-dependent translation. *Embo J.* 2009;28:58–68.
- [32] Skabkin MA, Kiselyova OI, Chernov KG, et al. Structural organization of mRNA complexes with major core mRNP protein YB-1. *Nucleic Acids Res.* 2004;32:5621–5635.
- [33] Pisarev AV, Skabkin MA, Thomas AA, et al. Positive and negative effects of the major mammalian messenger ribonucleoprotein p50 on binding of 40 S ribosomal subunits to the initiation codon of beta-globin mRNA. *J Biol Chem.* 2002;277:15445–15451.
- [34] Skabkin MA, Evdokimova V, Thomas AA, et al. The major messenger ribonucleoprotein particle protein p50 (YB-1) promotes nucleic acid strand annealing. *J Biol Chem.* 2001;276:44841–44847.
- [35] Snyder E, Soundararajan R, Sharma M, et al. Compound heterozygosity for Y box proteins causes sterility due to loss of translational repression. *PLoS Genet.* 2015;11:e1005690.
- [36] Kohno Y, Matsuki Y, Tanimoto A, et al. Expression of Y-box-binding protein dbpC/contrin, a potentially new cancer/testis antigen. *Br J Cancer.* 2006;94:710–716.
- [37] Tekur S, Pawlak A, Guellaen G, et al. Contrin, the human homologue of a germ-cell Y-box-binding protein: cloning, expression, and chromosomal localization. *J Andrology.* 1999;20:135–144.
- [38] Sears D, Luong P, Yuan M, et al. Functional phosphoproteomic analysis reveals cold-shock domain protein A to be a Bcr-Abl effector-regulating proliferation and transformation in chronic myeloid leukemia. *Cell Death Dis.* 2010;1:e93.
- [39] Matsumoto S, Uchiyama T, Tanamachi H, et al. Ribonucleoprotein Y-box-binding protein-1 regulates mitochondrial oxidative phosphorylation (OXPHOS) protein expression after serum stimulation through binding to OXPHOS mRNA. *Biochem J.* 2012;443:573–584.
- [40] Siegel PM, Massague J. Cytostatic and apoptotic actions of TGF-beta in homeostasis and cancer. *Nat Rev Cancer.* 2003;3:807–821.
- [41] Lyabin DN, Eliseeva IA, Skabkina OV, et al. Interplay between Y-box-binding protein 1 (YB-1) and poly(A) binding protein (PABP) in specific regulation of YB-1 mRNA translation. *RNA Biol.* 2011;8:883–892.
- [42] Skabkina OV, Lyabin DN, Skabkin MA, et al. YB-1 autoregulates translation of its own mRNA at or prior to the step of 40S ribosomal subunit joining. *Mol Cell Biol.* 2005;25:3317–3323.
- [43] Muller-McNicoll M, Rossbach O, Hui J, et al. Auto-regulatory feedback by RNA-binding proteins. *J Mol Cell Biol.* 2019;11:930–939.
- [44] Kemmerer K, Fischer S, Weigand JE. Auto- and cross-regulation of the hnRNPs D and DL. *RNA.* 2018;24:324–331.
- [45] Ran FA, Hsu PD, Wright J, et al. Genome engineering using the CRISPR-Cas9 system. *Nat Protoc.* 2013;8:2281–2308.
- [46] Glukhova KF, Marchenkov VV, Melnik TN, et al. Isoforms of green fluorescent protein differ from each other in solvent molecules 'trapped' inside this protein. *J Biomol Struct Dyn.* 2017;35:1215–1225.
- [47] Eliseeva I, Vasilieva M, Ovchinnikov LP. Translation of human beta-Actin mRNA is regulated by mTOR pathway. *Genes (Basel).* 2019;10:96.
- [48] Wakiyama M, Futami T, Miura K. Poly(A) dependent translation in rabbit reticulocyte lysate. *Biochimie.* 1997;79:781–785.
- [49] Presolski SI, Hong VP, Finn MG. Copper-catalyzed azide-alkyne click chemistry for bioconjugation. *Curr Protoc Chem Biol.* 2011;3:153–162.
- [50] Terenin IM, Andreev DE, Dmitriev SE, et al. A novel mechanism of eukaryotic translation initiation that is neither m7G-cap-, nor IRES-dependent. *Nucleic Acids Res.* 2013;41:1807–1816.
- [51] Guryanov SG, Filimonov VV, Timchenko AA, et al. The major mRNP protein YB-1: structural and association properties in solution. *Biochim Biophys Acta.* 2013;1834:559–567.
- [52] Gerashchenko MV, Gladyshev VN. Translation inhibitors cause abnormalities in ribosome profiling experiments. *Nucleic Acids Res.* 2014;42:e134.
- [53] Ingolia NT, Brar GA, Rouskin S, et al. The ribosome profiling strategy for monitoring translation in vivo by deep sequencing of ribosome-protected mRNA fragments. *Nat Protoc.* 2012;7:1534–1550.

- [54] Tenenbaum SA, Carson CC, Lager PJ, et al. Identifying mRNA subsets in messenger ribonucleoprotein complexes by using cDNA arrays. *Proc Natl Acad Sci U S A*. 2000;97:14085–14090.
- [55] Martin M. Cutadapt removes adapter sequences from high-throughput sequencing reads. *EMBnet.journal*. 2011;17:3.
- [56] Meyer LR, Zweig AS, Hinrichs AS, et al. The UCSC genome browser database: extensions and updates 2013. *Nucleic Acids Res*. 2013;41:D64–9.
- [57] Harrow J, Frankish A, Gonzalez JM, et al. GENCODE: the reference human genome annotation for the ENCODE project. *Genome Res*. 2012;22:1760–1774.
- [58] Dobin A, Davis CA, Schlesinger F, et al. STAR: ultrafast universal RNA-seq aligner. *Bioinformatics*. 2013;29:15–21.
- [59] Dunn JG, Weissman JS. Plastid: nucleotide-resolution analysis of next-generation sequencing and genomics data. *BMC Genomics*. 2016;17:958.
- [60] Robinson MD, McCarthy DJ, Smyth GK. edgeR: a Bioconductor package for differential expression analysis of digital gene expression data. *Bioinformatics*. 2010;26:139–140.
- [61] Sergushichev AA. An algorithm for fast preranked gene set enrichment analysis using cumulative statistic calculation. *BioRxiv*. 2016. doi:10.1101/060012
- [62] Subramanian A, Tamayo P, Mootha VK, et al. Gene set enrichment analysis: a knowledge-based approach for interpreting genome-wide expression profiles. *Proc Natl Acad Sci U S A*. 2005;102:15545–15550.